RESEARCH ARTICLE



Characterizing groundwater flow paths in an undeveloped region through synoptic river sampling for environmental tracers

Brian D. Smerdon¹ W. Payton Gardner²

Correspondence

Brian D. Smerdon, Department of Earth and Atmospheric Sciences, University of Alberta, Edmonton, AB T6G 2E3, Canada. Email: brian.smerdon@gmail.com

Abstract

Synoptic sampling of three rivers for a suite of environmental tracers is shown to be an efficient way to gain an understanding of groundwater flow paths for a previously unstudied large area in Alberta, Canada. For regional-scale characterization, classical hydrogeological techniques are limited by the location and number of groundwater wells. This study demonstrates that rivers can become an easily accessible location to sample the distribution of groundwater flow paths discharging to surface water. Modelling of groundwater discharge to the rivers and groundwater mean age helps generate knowledge of groundwater circulation for a large area, which is useful for conceptual model development and focusing future characterization efforts. Results indicate that the benchland areas in this region, with higher topographic relief, had hydrogeological conditions that favoured deeper groundwater circulation with a modelled mean age greater than 100 years from recharge to discharge. Lower relief areas, which coincide with a transition in bedrock formations in this region, appeared to have much shorter and shallower groundwater circulation. The approach required a field program completed in 5 days and financial budget approximately equivalent to drilling a single borehole and installing a monitoring well. It is concluded that under the right conditions, where few classical observation points exist and knowledge is limited, synoptic sampling of rivers can be used to develop scientifically defensible conceptual models at a comparable scale to regional planning and resource management.

KEYWORDS

baseflow, environmental tracers, geochemistry, groundwater, groundwater age, groundwater discharge, isotope

INTRODUCTION

Hydrogeological conceptual models bring together knowledge of the geological framework and the state of groundwater conditions, or groundwater regime as described by Tóth (1970). Together, these components establish the foundation for classifying groundwater systems in a region, aid the assessment of water availability and guide resource planning and future characterization needs. As a qualitative

interpretation, conceptual models are developed and refined based on a combination of observed data and insight about system behaviour (Bredehoeft, 2005; Enemark et al., 2019). Considering that many societal questions about water availability and management occur at a more regional-scale than site-specific assessments (Cools et al., 2006), scientifically defensible conceptual models at a comparable scale are needed that capture essential components of smaller spatial scales (Barthel, 2014).

¹Department of Earth and Atmospheric Sciences, University of Alberta, Edmonton, Alberta, Canada

²Department of Geosciences, University of Montana, Missoula, Montana, USA

To define a hydrostratigraphic framework at the regional scale, there are approaches to bring together multiple data types (Allen et al., 2008; Dunkle et al., 2015) and create detailed 3D geocellular models (MacCormack et al., 2019; Moya et al., 2014). Computing software is continually advancing to support the inclusion of a wide range of information and varying degrees of heterogeneity, which in-turn facilitates richly detailed and informative hydrostratigraphic models (Babakhani et al., 2019; Lekula et al., 2018). Airborne geophysical methods have also proven to be insightful when mapping hydrostratigraphic units across large areas (Knight et al., 2018), although data acquisition can require significant financial resources (Jørgensen et al., 2013). Earth observation techniques, such as the Gravity Recovery and Climate Experiment satellite mission, have provided global and national scale assessments of the groundwater regime (Frappart & Ramillien, 2018). Although initial applications were for very large areas, the gap between the spatial scale of remote-sensing and monitoring well observations is closing (Huang et al., 2016; Knappe et al., 2019: Stampoulis et al., 2019).

If the goal of hydrogeological conceptualization is to define the geometry of a groundwater flow system in a region (Tóth, 1970), we wonder if similar approaches exist to define groundwater flow paths at the same scale as used in hydrostratigraphic modelling. Classical hydrogeological techniques, based on analysis of hydraulic heads and groundwater chemistry, are typically limited by the location and number of groundwater wells or springs. These traditional forms of subsurface data acquisition (e.g. drilling, well installation and groundwater sampling) are costly, especially for a regional application where a multitude of observations points are needed. However, under the right conditions, rivers can become an easily accessible location to sample the distribution of groundwater flow paths discharging to surface water (Cook, 2015; Gardner et al., 2011; Smerdon et al., 2012), especially in remote regions where there may be few classical observation points (Batlle-Aguilar et al., 2014). The nature of baseflow can generally be related to geology (Bloomfield et al., 2009) and the concentrations of multiple environmental tracers may encode information on the provenance of groundwater (Solomon et al., 2010), rate of circulation through the hydrogeological system (Stolp et al., 2010) and interaction with surface water (Cook et al., 2006). From a regional perspective, rivers may contain much of what is needed to generate knowledge of the state of groundwater conditions.

The objective of this study is to characterize groundwater flow paths of a large region through synoptic sampling of rivers for environmental tracers. At the time of this investigation, very little was known about the hydrogeology for the area of interest, except the basic physiographical and geological setting and few long-term hydrometric stations. A tracer-based approach was chosen based on the capability to identify different sources of water providing baseflow to rivers and infer something about the groundwater conditions in a region (Jasechko, 2016; Solomon et al., 2015), assuming that active groundwater flow systems discharge to the rivers. For the tracerbased approach, the river water represents the flow-weighted average concentration of tracers in groundwater within the region. Similar to using 'unconventional observations' to improve a numerical

groundwater model (Schilling et al., 2019), this study uses synoptic sampling results to efficiently gain a conceptual understanding of a region that had not been previously investigated.

MATERIALS AND METHODS 2 |

2.1 Study site

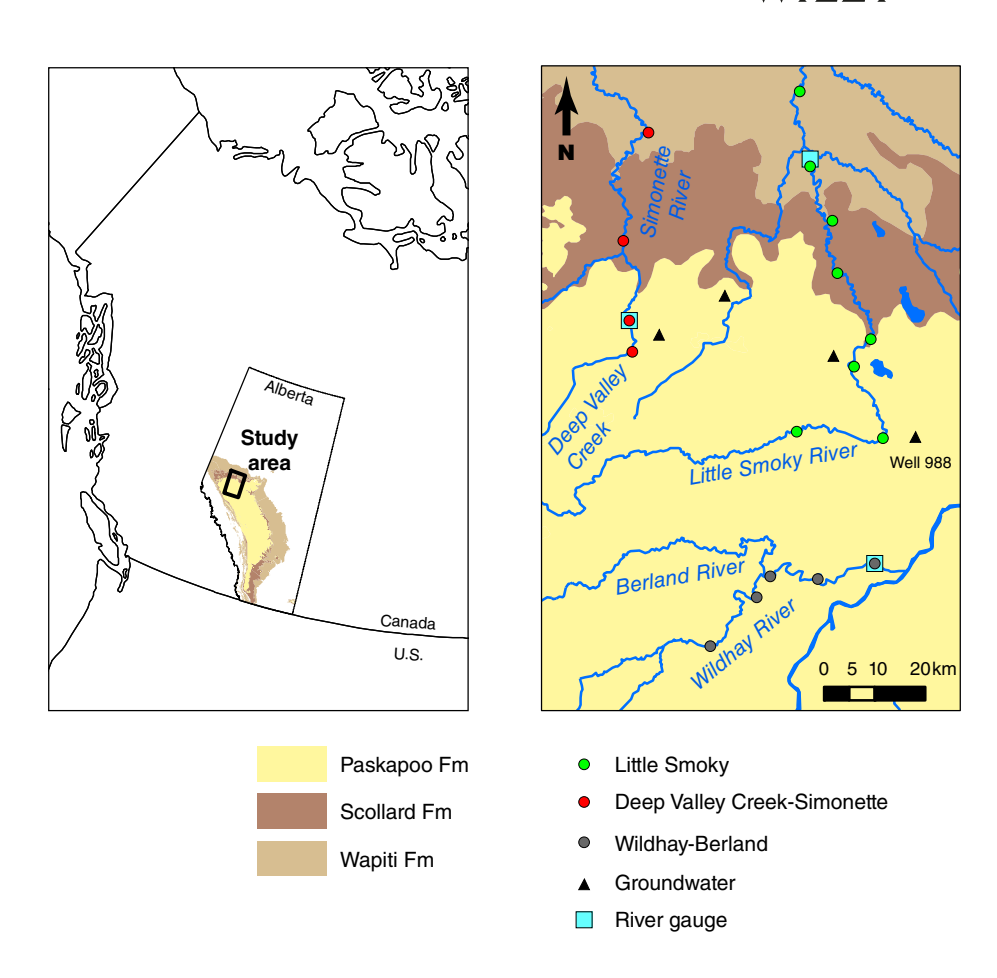
The region of investigation is located in Alberta, Canada (Figure 1), with nearly 95% of the landscape being forested, relatively unpopulated and containing infrastructure to support oil and gas production (e.g. roads, well pads) and the forestry industry. The region encompasses active shale gas plays (Montney and Duvernay formations), which have required water to support development since 2012 for activities such as hydraulic fracturing (Alessi et al., 2017). A lack of knowledge regarding the local to regional groundwater system and its interaction with surface water provided the impetus for investigation in this region.

The climate of the region varies spatially. The 1981–2010 climate normals (Wang et al., 2016) for the southern portion of the region were 680 mm/year for precipitation and 500 mm/year for reference evaporation, indicating an average water surplus of 180 mm/year. In the northern portion of the region, climate normals were 505 mm/ year for precipitation and 560 mm/year for reference evaporation, indicating an average water deficit of 55 mm/year. As shown in Figure 1, there are three river gauging stations in the region (Environment and Climate Change Canada, 2018), which guided the sampling program used in this study; however, there is only one publicly available groundwater monitoring well (well no. 988: Alberta Environment and Parks, 2019).

The physiography includes benchlands of moderate topographic relief (100-200 m) with river valley incisions, and lower relief plains to the north and southeast. The thickness of sediment above bedrock is variable (Atkinson & Hartman, 2017), with up to 5 m of glaciogenic diamict with an abundance of gravel in the benchlands and 25-40 m of glaciogenic diamict with finer grained materials in the plains. The Upper Cretaceous-Paleogene bedrock formations in the region consist of the Wapiti, Battle, Scollard and Paskapoo formations (listed from oldest to youngest), which all subcrop toward the north (Figure 1).

The Wapiti Formation consists of a lower siltstone and sandstone unit and upper interbedded mudstone and sandstone (Dawson et al., 1994). This bedrock unit is quite thick in the region (up to 1000 m) and has not been formally subdivided; however, Fanti and Catuneanu (2009) suggest that the Wapiti Formation may have five distinct stratigraphic units corresponding to significant changes in major drainage systems during the Cretaceous. The Battle Formation is a mudstone (Irish, 1970) and is relatively thin (about 10 m thick) or eroded entirely in many places (Hathway, 2011). The Scollard Formation consists of sandstone and siltstone, interbedded with mudstone (Dawson et al., 1994), also having extensive coal seams. This bedrock unit is up to 400 m thick in the southwest portion of the study area and thins toward the subcrop margin.

FIGURE 1 Location of the study area and water sampling sites (rivers, groundwater) shown with Upper Cretaceous–Paleogene bedrock formations in Alberta, Canada



The Paskapoo Formation is a siltstone and mudstone and interbedded with high permeability coarse-grained channel sandstone (Grasby et al., 2008; Hamblin, 2004). In the study area, the Paskapoo Formation varies in thickness from 850 m in the southwest, to 10's of meters (or less) in the north where it subcrops. It is the uppermost bedrock formation across much of central and southern Alberta as shown on Figure 1, highly heterogeneous (Hughes et al., 2017), with sandstone units that form important local to regional scale aquifers in the Canadian Prairies (Grasby et al., 2014). Given the potential significance as a groundwater source and heterogeneity, several geostatistical studies have focused on the Paskapoo Formation to map sandstone abundance, either in specific areas (Babakhani et al., 2019; Burns et al., 2010; Quartero et al., 2015) or across the entire formation (Lyster & Andriashek, 2012; Mei, 2019). The study by Babakhani et al. (2019) was completed concurrently with our tracer investigation and was focussed on bedrock formations in the same region. This allows discussion of our findings in relation to a detailed model of sandstone abundance, which can be considered a proxy for transmissivity.

2.2 | Water sampling

Field investigation focused on three river systems, including the Little Smoky River, the Deep Valley Creek-Simonette river system, and Wildhay-Berland river system. Two of the river systems comprise tributaries that merge within the study area, with Deep Valley Creek joining the Simonette River and the Wildhay River joining the Berland River (Figure 1). Selection of these river systems was based on the river traversing different subcropping bedrock formations and the presence of a hydrometric gauging station operated by Environment Canada (gauge locations shown on Figure 1). For the Wildhay-Berland river system, there was also a potential variation in sandstone abundance determined at the formation scale (Lyster & Andriashek, 2012) that had not been confirmed by field investigation.

River sampling was completed in September 2015 when the rivers were close to their low flow state, which was similar to the fifth percentile of discharge (i.e. Q_{95}) based on the period of record (33–52 years depending on location). River samples were collected on a 170 km segment of the Little Smoky River, and 75 km segments of the Deep Valley Creek–Simonette river system and Wildhay–Berland river system. The distance between sample locations varied from 10 to 40 km, depending on access to the rivers by roads and trails. Water samples were collected approximately 3 m from the riverbank using a peristaltic pump with the intake tubing located just above the riverbed. At the time of sample collection, field parameters including pH, water temperature and specific conductance were measured. Groundwater from the Paskapoo Formation was sampled at four locations (Figure 1). Three locations were opportunistically sampled in March 2015 from private water wells with depths from 24 to 41 m

being used by oil and gas companies for their operations. These wells were pumping at the time of sampling, so groundwater was sampled after measurements of temperature, electrical conductivity and pH appeared stable for the pumping rate at the time of sampling. The single publicly available groundwater monitoring well with a depth of 108 m was sampled in March 2018 as part of on-going monitoring by the Alberta government. As this well contains a low volume of water, no purging was done and the sample was acquired using a discrete sampler.

Major ions, alkalinity and the isotopic tracers were measured on all samples except the single publicly available groundwater monitoring well, which was not analysed for ²²²Rn, SF₆ or noble gases. Dissolved major ions and alkalinity were analysed by a commercial laboratory in Edmonton, Alberta. Stable isotope ratios (δ^{18} O and δ^2 H) were measured at the Department of Earth and Atmospheric Sciences at the University of Alberta (Edmonton, Alberta) with a Picarro wavelength-scanned cavity ring-down spectroscopy and expressed as δ values representing deviations in per mil from Vienna standard mean ocean water (VSMOW). 222Rn was measured at the end of each day in the field on water samples collected in 250 ml glass bottles using a RAD7 radon detector (Durridge Company, Inc.). SF₆, ³H and noble gases (Ar, Kr, Xe, Ne and ⁴He) were measured by Dissolved and Noble Gas Service Center at the University of Utah (Salt Lake City, UT). SF₆ was analysed by gas chromatography with electron capture detector, ³H was analysed by He ingrowth method, and noble gases were collected in copper tubes and analysed by mass spectrometery.

2.3 | River transport modelling

The rate of groundwater discharge to the rivers and groundwater mean age were estimated by solving a series of equations sequentially. First, the downstream distribution of groundwater discharge was estimated by fitting the measured ²²²Rn concentration and the observed river discharge (Cook et al., 2006). With this approach, gauged river discharge represents a volumetric integration of water sources (including groundwater inflow) and variation in ²²²Rn is used to interpret downstream changes of groundwater inflow. Second, the groundwater mean age was estimated using a lumped parameter model that calculates the concentration of environmental tracers in discharging groundwater as a function of the groundwater residence time distribution (Maloszewski & Zuber, 1982). For the river transport modelling, we assume the rivers to be well mixed, such that each river sample represents a flow-weighted mean concentration.

2.3.1 | Groundwater discharge

The 1D river transport model described by Cook et al. (2006) includes: advection, dispersion, gas exchange, first-order decay and groundwater inflow. Derivation of the equations describing longitudinal concentrations of environmental tracers in a river and the underlying

assumptions are presented in Appendix S1. River discharge (Q) is described in terms of inflows and outflows (Equation 1).

$$\frac{\partial Q}{\partial x} = Pw - Ew + \frac{Q_T}{\Delta x} - \frac{Q_Q}{\Delta x} + q_{gi}w - q_{go}w, \tag{1}$$

where P is precipitation, E is evaporation, Q_T is tributary discharge, Q_Q is pumping, q_{gi} is groundwater inflow, q_{go} is groundwater outflow, x is distance and w is river width. Longitudinal concentration of an environmental tracer in the river (C) is described in terms of advective-diffusive transport (Equation 2).

$$\frac{\partial C}{\partial x} \!=\! \frac{A}{Q} \! \left(\frac{\partial}{\partial x} D \frac{\partial C}{\partial x} \right) + \frac{q_{giW}}{Q} (C_{GW} - C) + \frac{Q_T}{\Delta x Q} (C_T - C) - \frac{kw}{Q} (C - C_{ATM}) - \frac{A}{Q} \lambda C, \eqno(2)$$

where D is the longitudinal hydrodynamic dispersivity, A is the river cross-sectional area, $C_{\rm GW}$ is the approximate local groundwater concentration, k is the gas exchange velocity for each tracer, $C_{\rm ATM}$ is the atmospheric equilibrium concentration, λ is the decay coefficient and C_T is the approximate concentration of the tributary.

Equations (1) and (2) were solved numerically using the method described by Beisner et al. (2018). Lateral groundwater discharge to the rivers was estimated by fitting measured concentrations of 222 Rn and river discharge and modifying the spatially distributed groundwater inflow as segments. In order to reduce non-uniqueness and avoid over-fitting and/or aliasing of groundwater signals, the groundwater inflow was assumed to follow a step function, with n equal steps, where n is equal to the number of 222 Rn sampling points along each river. Thus, we solve for n groundwater inflow values, given n 222 Rn observations and known discharge measurements. Inversion for optimal groundwater inflow was performed using a Marquart–Levenberg optimization routine, which minimized an uncertainty-weighted chisquared residual.

2.3.2 | Groundwater mean age

For environmental tracers indicative of water age, C_{GW} is described by the convolution integral, assuming a residence distribution (Equation 3; Maloszewski & Zuber, 1982).

$$C_{\text{GW}}(t) = \int_{0}^{\infty} C_{\text{IN}}(t - \tau)g(\tau)e^{-\lambda t}d\tau, \qquad (3)$$

where t is the time of observation, τ is the residence time from recharge to the sampling point and $g(\tau)$ is the assumed residence time distribution. The residence time distribution $g(\tau)$ is a function of the flow system configuration and has been analytically derived for several different aquifer configurations. Here, we consider two end member age models that account for a large spectrum of aquifer configurations (Leray et al., 2016; Maloszewski & Zuber, 1982). The exponential model is representative of equal mixing of all flow paths

from zero to infinite age, having a mean residence of τ_m , and represents well-mixed discharge from an unconfined aquifer with a large distribution of flow paths (Equation 4).

$$g(\tau) = \frac{1}{\tau_m} e^{-\frac{\tau}{\tau_m}}.$$
 (4)

The dispersion model is representative of a single groundwater flow path subject to dispersive mixing, where the amount of dispersion is characterized by the Peclet number (P_e ; Equation 5).

$$g(\tau) = \tau^{-1} \left(\frac{4\pi P_e \tau}{\tau_m} \right)^{-\frac{1}{2}} e \left(-\frac{\tau_m \left(1 - \frac{\tau}{\tau_m} \right)^2}{4P_e \tau} \right). \tag{5}$$

Different residence time distributions will result in a different expected groundwater concentration given the same mean residence time, thus the assumption of the residence distribution is fundamental. In groundwater age dating studies, it is common to use an observed groundwater concentration ($C_{\rm GW}(t)$) and the known historical input function ($C_{\rm IN}(t-\tau)$), and solve Equations (3)–(5) in an inverse manner to estimate the mean groundwater residence time.

In this study, a single mean age of groundwater for an assumed groundwater age distribution was estimated by fitting the river SF₆ and ³H concentrations using Equations (3)-(5), once an estimate of groundwater discharge was made. Focusing on the river concentrations rather than groundwater sampled from individual water wells helped begin to understand groundwater circulation in the region since the rivers integrate different sources of water, including baseflow. The modelled mean age of groundwater discharge was estimated through a Marguart-Levenberg minimization of the errorweighted chi-squared residual of observed and modelled river SF₆ and ³H concentration. At the same time, ⁴He concentration and stable isotopes in the river were modelled for comparison and validation. The ⁴He concentration represents a combination of helium from equilibration with the atmosphere, helium added from radioactive decay of subsurface materials (i.e. a radiogenic source), and the possibility of helium generated separate from the groundwater reservoir (e.g. mantle-derived). We assume that any variation in ⁴He concentration would largely be caused by radiogenic addition occurring as groundwater moves along a flow path. Because we are interested in a general conceptual model of the groundwater systems, we assume that modelled mean groundwater age is spatially constant (i.e. a single mean age for all groundwater discharge in each river system).

2.3.3 | Modelling parameters

A summary of parameters can be found in Table 1, which were selected to be generally representative of each river system and the few measured groundwater concentrations determined in the study

area. The river geometry (width and depth), approximate tributary discharge, and summary of river discharge statistics can be found in Appendix S2. The river width and depths were estimated at each sampling location, and tributary inflow (Q_T) was approximated using Google Earth imagery and the size of the tributary compared to the gauged river systems. Discharge statistics for each river system include Q_{50} , Q_{95} and Q_{\min} available for the period of record as well as the observed discharge at the time of sampling. During the sampling period, pumping (Q_Q) was negligible and set to zero.

For ²²²Rn, the atmospheric equilibrium concentration was set to zero. For ⁴He and SF₆, the atmospheric concentration was calculated as the Henry's law equilibrium concentration using the maximum elevation and temperature for the river, which gives the minimum atmospheric equilibrium concentration. Henry's coefficients were calculated using equations from Ballentine et al. (2002) and references therein. Gas exchange coefficients for ²²²Rn and ⁴He were specified using the river channel width, depth, discharge and slope and river temperature after Raymond et al. (2012). The longitudinal hydrodynamic dispersivity (D) was set to zero, which for the fully implicit numerical solution means that dispersive flux is controlled by the grid cell spacing (Beisner et al., 2018).

The historical input of 3 H (Figure 2a) and stable isotopes was taken from the precipitation record in Ottawa, Canada (IAEA/WMO, 2016). The historical input of SF₆ in the atmosphere (Figure 2a) was taken from National Oceanic and Atmospheric Administration, Global Monitoring Division, northern hemisphere averages (NOAA, 2018). Groundwater concentrations for 222 Rn, δ^2 H, δ^{18} O and 4 He were set to the average value measured in groundwater wells sampled in the study area (Table 1).

3 | RESULTS

3.1 | Water analyses

River water samples had a narrow pH range of 8.4–8.8 and temperature range of 7.0–13.0°C, whereas groundwater samples had slightly lower pH values (6.9–8.5) and temperature (4.3–6.5°C). For river water, TDS values were less than 250 mg/L, with some differences between each of the river systems. The TDS values varied from 161 to 192 mg/L for the Little Smoky River, from 180 to 220 mg/L for the Deep Valley Creek–Simonette river system, and from 228 to 248 mg/L for the Wildhay–Berland river system. There was a subtle downstream increase in TDS for the Little Smoky and Deep Valley Creek–Simonette river systems, which span three different bedrock formations (Figure 1). There was also a subtle downstream decrease for the Wildhay–Berland river system, which passes through a single formation having variability in sandstone abundance. From the limited groundwater sampling, TDS was found to vary from 378 to 600 mg/L.

The stable isotope ratios of water are shown on Figure 3 relative to a local meteoric water line (LMWL: $\delta^2H=7.25~\delta^{18}O$ – 11.37) and an adjusted local evaporation line (LEL: $\delta^2H=4.12~\delta^{18}O$ – 71.34)



TABLE 1 Modelling parameters for each river system

			Value for each river system		
Parameter	Description	Source	Little Smoky	Deep Valley Creek- Simonette	Wildhay- Berland
Т	River temperature (°C)	Measured in this study; maximum of river temperatures	13	11.2	12.4
Z	Average elevation (masl)	Measured in this study; maximum of sampling locations	950	870	1010
$T_{\sf GW}$	Groundwater recharge temperature (°C)	Measured in this study; average of sampled groundwater temperature	4.8	4.8	4.8
Z_{GW}	Groundwater recharge elevation (masl)	Measured in this study; average of sampled groundwater elevation	878	878	878
E	Evaporation rate (mm/day)	Estimated	2	2	2
k _{Rn}	Gas exchange velocity: ²²² Rn (m/day)	Raymond et al. (2012); Equation (7)	0.587	1.48	1.77
k _{SF6}	Gas exchange velocity: SF ₆ m/day)	Raymond et al. (2012); Equation (7)	0.575	1.45	1.73
k _{He}	Gas exchange velocity: ⁴ He (m/day)	Raymond et al. (2012); Equation (7)	1.8	3.9	4.6
λ	Decay coefficient: ²²² Rn (/day)	Cook and Herczeg (2000)	3.82	3.82	3.82
t _{1/2}	Half-life: ³ H (year)	Cook and Herczeg (2000)	12.32	12.32	12.32
Pe	Peclet number for dispersion	Representative value with advection slightly more important than dispersion	2	2	2
C_{GW-Rn}	Average groundwater concentration: ²²² Rn (Bq/L)	Smerdon et al. (2019)	7.62	7.62	7.62
C _{GW-δ¹⁸O}	Average groundwater concentration: $\delta^{18}O$ (%)	Smerdon et al. (2019)	-19.7	-19.7	-19.7
$C_{GW\text{-}\delta^2H}$	Average groundwater concentration: δ^2H (‰)	Smerdon et al. (2019)	-153.9	-153.9	-153.9
C _{GW-⁴He}	Average groundwater concentration: ⁴ He (ccSTP/g)	Smerdon et al. (2019)	1.1E-7	1.1E-7	1.1E-
C_{GW-SF_6}	Average groundwater concentration: SF ₆ (fMol/kg)	Smerdon et al. (2019)	0.03	0.03	0.03
C _{GW-3} H	Average groundwater concentration: ³ H (TU)	Smerdon et al. (2019)	1.9	1.9	1.9

developed for the Utikuma Region Study Area, which is located 225 km northeast of the study area (Hokanson et al., 2019). The slope of the LEL remains the same as Hokanson et al. (2019) with an arbitrary 5% decrease in $\delta^2 H$ intercept to provide context for river water results. Results for the Little Smoky River plot along the adjusted LEL and increase with downstream distance (–18.5 to –17.4% and –147.8 to –142.5% for $\delta^{18} O$ and $\delta^2 H$, respectively; Figure 4), whereas samples from the Wildhay–Berland (mean of –19.1% $\delta^{18} O$ and –151.3% $\delta^2 H$) and Deep Valley Creek–Simonette (mean of –18.6% $\delta^{18} O$ and –147.4% $\delta^2 H$) river systems plot more tightly together along the LMWL. Groundwater samples were found to have –19.2 to –20.2% and –157.7 to –149.9% for $\delta^{18} O$ and $\delta^2 H$, respectively.

Figure 4 shows the results of river sampling for most of the isotopic tracers in this study. For each river, the distance is relative to the initial sampling location. 222 Rn in the rivers was low and varied from 0.05 to 0.32 Bq/L, with most values close to the average of 0.17 Bq/

L. In groundwater samples 222 Rn varied from 7.6 to 25.1 Bq/L. Similar to TDS, 222 Rn was found to be higher for the Deep Valley Creek–Simonette and Wildhay–Berland river systems than the Little Smoky River. The concentration of 4 He was found to be in the order of 4E-8 ccSTP/g for the river samples, and 6E-8 to 2E-7 ccSTP/g for the groundwater samples.

Values for 3 H and SF $_6$ in the rivers varied from 6.7 to 9.0 tritium units (TU) and 0.34 to 0.42 pg/kg (2.3–3.2 fMol/kg), respectively. Similar to the TDS values, the longitudinal concentration of isotopic tracers is distinct for each river system and will be discussed with the river transport modelling results. For groundwater, 3 H and SF $_6$ concentrations were 0.1–4.5 TU and 0.007–0.073 pg/kg (equivalent to 0.1–0.9 fMol/kg or 0.1–1.4 pptv), respectively (Figure 2b). While isotopic tracer data for groundwater are sparse, two of the three groundwater samples had low 3 H concentrations and very low SF $_6$ concentrations.

FIGURE 2 (a) Historical concentrations of 3 H representative of Ottawa, Ontario (IAEA/WMO, 2016) decay-corrected to 2015 and SF₆ representative the northern hemisphere average (NOAA, 2018). (b) 3 H and SF₆ results for river and groundwater

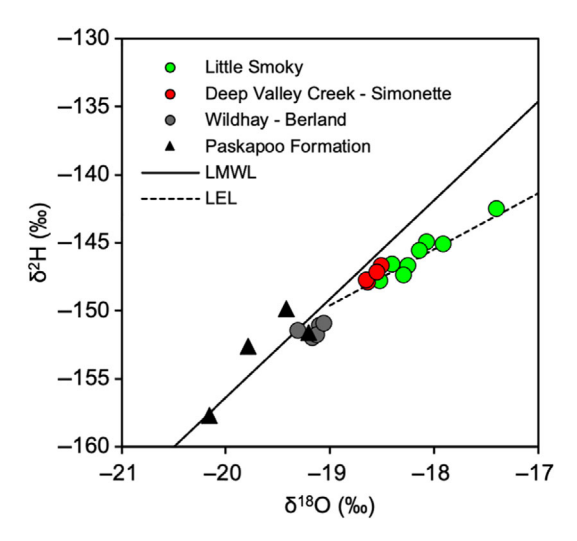


FIGURE 3 Stable isotope values ($\delta^2 H$ and $\delta^{18}O$) for river and groundwater samples relative to the local meteoric water line (LMWL) developed by Hokanson et al. (2019) for a research site located 225 km northeast of the study area. The slope of the local evaporation line (LEL) is the same as reported by Hokanson et al. (2019) with a 5% decrease in $\delta^2 H$ intercept to illustrate the potential evaporative effect on rivers in the study area

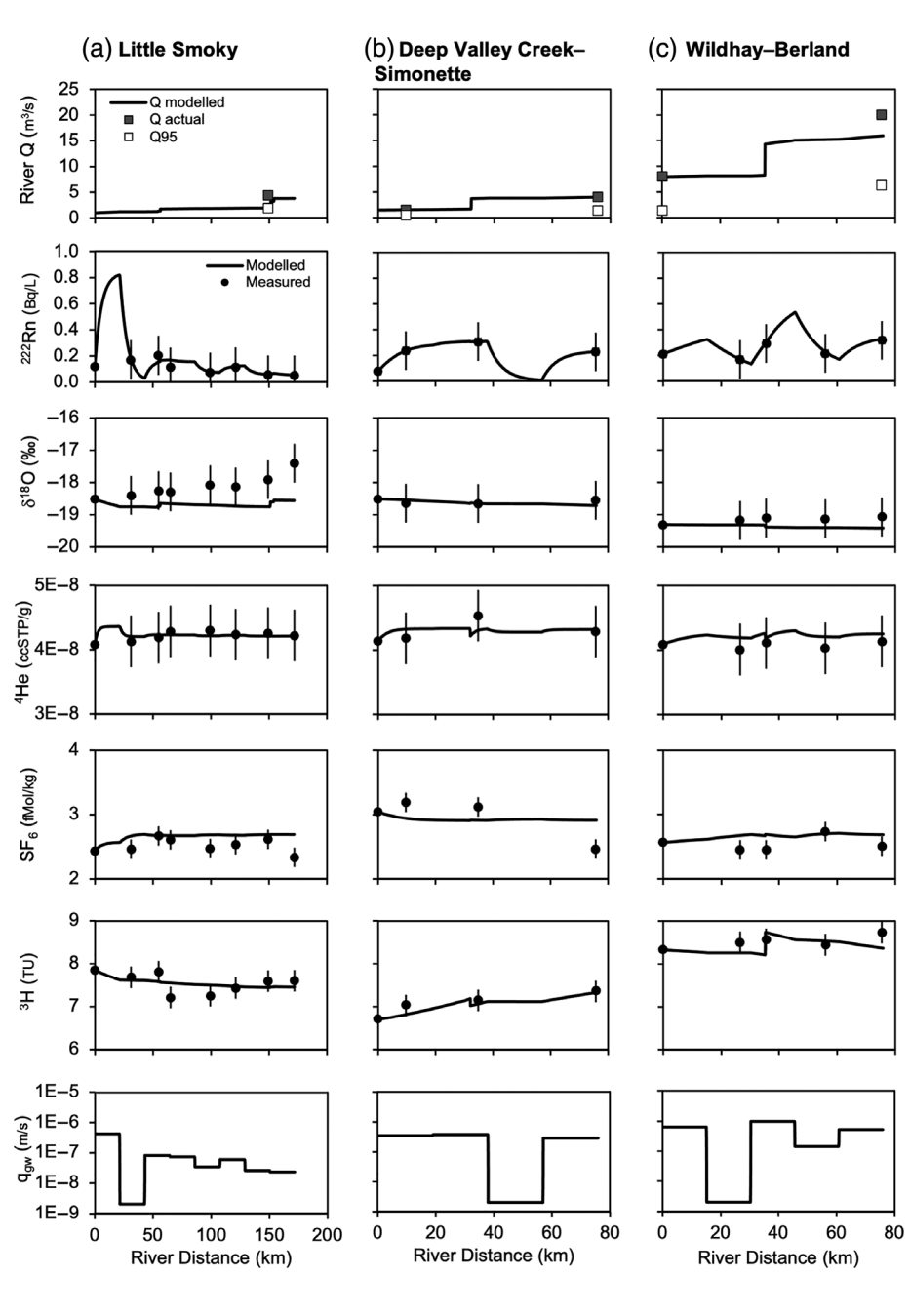
3.2 | River transport modelling

Figure 4 also shows the results of river transport modelling. The modelled groundwater discharge flux to obtain the best fit to measured concentration of 222 Rn is shown for segments of each river system. For comparison, the actual river flow (Q_{actual}) at the time of sampling is shown with the long-term low flow (Q_{95}) for the month of September. Relatively small but abrupt step increases in river flow are due to the assumed inflow from tributaries (shown in Supporting Information S2).

For the Little Smoky River (Figure 4a), the groundwater discharge flux was generally low (4.1E-7 m/s or less), with the majority of discharge occurring within the first 50 km of the sampled reach. This inflow of groundwater drives an increase in modelled ²²²Rn and ⁴He that could be further explored in more refined river sampling with smaller river segments. The lowest groundwater discharge section of the Little Smoky River was found between 25 and 40 km, where groundwater discharge was found to decrease below 1E-8 m/s. For the Deep Valley Creek-Simonette river system (Figure 4b), groundwater discharge was 3E-6 m/s across most of the sampled reach, except for between 38 and 57 km, where it was to less than 1E-8 m/s. For the Wildhay-Berland river system (Figure 4c), groundwater discharge was variable throughout the portion of the river that was sampled. Discharge was found to be greater than 1E-9 m/s along the entire portion of the river that was sampled, with sections from 0 to 15 km, 30 to 45 km and 60 to 75 km having groundwater discharge above

Using the historic input of SF_6 and 3H concentrations (Figure 2a) and observed SF_6 and 3H concentrations in the river (Figure 4), the best fit exponential and dispersion model mean ages were calculated for all three rivers and are summarized in Table 2. For both the Little Smoky and Wildhay–Berland rivers, the best fit modelled mean age of groundwater discharge was greater than 100 years for both age distributions. The Deep Valley Creek–Simonette, showed an estimated age of ranging between 9 and 21 years. The older modelled mean ages agree with the limited results for isotopic tracers in groundwater samples that showed low but detectable concentrations of SF_6 and 3H (Figure 2b), and slightly higher 4He .

The overall fit of the environmental tracer modelling with respect to the estimated analytical error variance of the samples can be quantified with the reduced chi-squared residual. A reduced chi-squared residual of 1 indicates a model that fits the observations at the expected analytical error variance. Chi-squared residuals much greater



river discharge (top row) and concentrations of isotopic tracers in river water for the modelled rate of groundwater discharge into each river (bottom row). Groundwater discharge was determined by fitting both ²²²Rn concentration and river discharge. Error bars are calculated from the average estimated analytical and sampling reproducibility

 TABLE 2
 Summary of mean age of groundwater discharge for each river system

River system	Bedrock formation	Exponential mean age (years)	Reduced chi squared	Dispersion mean age (years)	Reduced chi squared
Little Smoky	Paskapoo, Scollard, Wapiti	100.3	0.48	117.8	0.48
Deep Valley Creek- Simonette	Paskapoo, Scollard, Wapiti	20.7	2.01	8.6	2.01
Wildhay-Berland	Paskapoo	145.7	1	138	0.96

than 1 indicate a poor fit and chi-squared residuals much less than 1 indicate over-fitting (i.e. fitting expected error). Our inversion results for mean age show moderately good performance ranging in from 0.48 for the Little Smoky and up to 2 for the Deep Valley

Creek–Simonette, with an average chi squared for all models of 1.17. In general, the model fits appear to be reasonable; however, Little Smoky model is likely over-fitting (or we have over-estimated the analytical error variance) and the Deep Valley Creek–Simonette

on Wiley Online Library for rules of use; OA articles are governed by the applicable Creative Common

WILFY 9 of 15

is under-fitting (or we under-estimated the analytical error variance).

4 | DISCUSSION

4.1 | Synoptic sampling approach

Synoptic river sampling studies have often been used to examine the interaction of groundwater and surface water, including locating segments of discharge (Lee & Hollyday, 1991), estimating the exchange fluxes (Cook et al., 2006) and identifying the age of baseflow sources (Solomon et al., 2015; Stolp et al., 2010). In some cases, the experimental approach is driven by a specific hydrological observation needing closer examination. For example, Gardner et al. (2011), Smerdon et al. (2012) and Beisner et al. (2018) focused on highly gaining segments of rivers and estimated the influence of old groundwater. Often, to generate knowledge of a broader region, additional information is required. For example, McCallum et al. (2012) incorporated differential flow gauging to reduce the uncertainty of groundwater discharge modelling, and Harrington et al. (2014) incorporated airborne geophysics to better define the subsurface heterogeneity associated with a key discharge zone. Synoptic river sampling studies are seldom used to characterize groundwater conditions without Supporting Information. The only study we are aware of that characterized a large region solely using a synoptic sampling approach is Batlle-Aguilar et al. (2014), who completed a large sampling campaign on a single river (400 km length) to understand groundwater inflows to a remote tropical region.

Similar to Batlle-Aguilar et al. (2014), we were only guided by preexisting mapping of the bedrock geology and a hydrometric station on each of the rivers in the current study. At the time of our field investigation, very little was known about the groundwater regime; however, the timing of sampling occurred when the rivers were close to a condition similar to Q_{95} (Supporting Information S2). Under relatively low flow conditions, our approach was to develop first-order knowledge of the groundwater regime by investigating the composition of river water using multiple environmental tracers. With a suite of environmental tracers aimed at detecting variations in mean water age, the goal was to learn as much as possible through a relatively short field campaign (similar to Batlle-Aguilar et al., 2014). The sampling was completed in just 5 days with the sum of laboratory analyses fees approximately equivalent to drilling a single borehole and installing a monitoring well.

The river sampling approach of this study requires consideration of the length scale for the various environmental tracers compared with the sampling interval (Cook, 2015). Changes to the input of a tracer to a river will only be detected for a limited distance downstream until equilibration with the atmosphere or decay occurs. For the environmental tracers used here, the length scales vary from approximately 10 to 40 km, similar to the sampling intervals. There will be situations where a tracer with a shorter length scale (e.g. 10 km) is sampled at a greater interval (e.g. >10 km). This could

potentially mask some of the lateral variation, which in-turn would not be accounted for when modelling groundwater discharge to the river. Where these situations occur, or modelling suggests significant change in a tracer concentration, supplementary sampling could be used to refine interpretation of groundwater discharge.

4.2 | Role of geological setting

Using the discharge statistics for each hydrometric station, specifically Q_{50} and Q_{min} , (shown in Appendix S2) we can calculate the proportion of minimum recorded discharge compared to the median discharge (i.e. Q_{\min}/Q_{50}) as an approximation of the base flow index (BFI) described in Gustard et al. (1992). Q_{min}/Q_{50} values close to zero would indicate low baseflow proportion (i.e. a flashy river) and values close to 1 would indicate high baseflow proportion. While BFI is more accurately defined by analysing daily mean and minimum discharge, the approach here is a relative comparison of each river for hydrometric stations that have operated for 52 years on the Little Smoky River and 33 years on the Wildhay-Berland and Deep Valley Creek-Simonette river systems. The Q_{min}/Q_{50} values are 0.21 for the Little Smoky River, 0.26 for the Deep Valley Creek-Simonette river system, and 0.43 for the Wildhay-Berland river system. The approximations would suggest that the Wildhay-Berland river system has a slightly higher proportion of baseflow and likely receiving groundwater from more permeable geological formations.

The stable isotope results indicate that the Wildhay–Berland river system is very similar to the stable isotopes of groundwater in the Paskapoo Formation, corroborating a higher proportion of baseflow. Both the Little Smoky River and the Deep Valley Creek–Simonette river system have stable isotopic conditions that are similar to the LEL (Figure 3); however, the isotopic values for the Little Smoky River are increasing in the downstream direction (Figure 4). These data align with slightly lower Q_{\min}/Q_{50} values suggesting less influence of groundwater on the river isotopic composition. Interestingly, the modelled isotopic compositions for the Little Smoky River, which consider groundwater discharge only and no evaporative fractionation, show a downstream bias (Figure 4). River transport modelling provides an estimation of variation in groundwater discharge, and also found that two of the three rivers in this region have groundwater discharge with a modelled mean age greater than 100 years.

To begin developing a conceptual hydrogeological model, the results of the tracer sampling and river transport modelling can be interpreted along with the background knowledge of the physiography and formation scale bedrock geology. Where the landscape has higher relief (e.g. benchlands), the river valleys have greater incision that generates greater hydraulic potential and drives deeper groundwater circulation. Where the landscape has lower relief also coincides with a transition to more mudstone and siltstone dominated bedrock with less river incision. Groundwater discharge to the rivers is diminished in these low relief areas, and younger groundwater discharge likely originates from adjacent alluvial aquifers (e.g. 9-21 year modelled mean age for the Deep Valley Creek–Simonette river system).

Landscape relief in the study area is caused by river incision, which inturn governs aquifer thickness and influences the groundwater catchment size (Haitjema, 1995). The net effect for these rivers is that landscape relief influences the flowpath length and depth of baseflow source (Welch & Allen, 2012).

Additional geological data (sandstone abundance modelling; Babakhani et al., 2019) that was developed concurrently to our tracer sampling program helps demonstrate this relation between bedrock geology and groundwater circulation (Carlier et al., 2019). Figure 5a depicts modelled sandstone abundance of the uppermost 50 m of bedrock and results of the river transport modelling, colour coded to order-of-magnitude groundwater discharge rates from Figure 4. From the regional perspective, we see that higher groundwater discharge predicted by the tracer sampling approach is often found near higher sandstone abundance, as expected. Where the sandstone abundance is lower, groundwater discharge predicted by the tracer sampling approach is also low. This comparison provides some indication that changes in modelled groundwater discharge reflect different patterns of groundwater circulation and the varying productivity of such a heterogenous bedrock formation (Grasby et al., 2008).

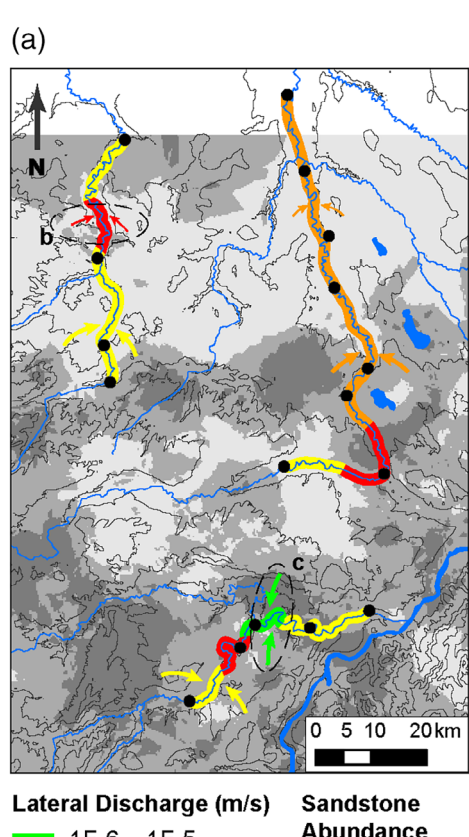
Combined with the bedrock geology, there are key physiographic attributes that influence groundwater circulation (Carlier et al., 2019),

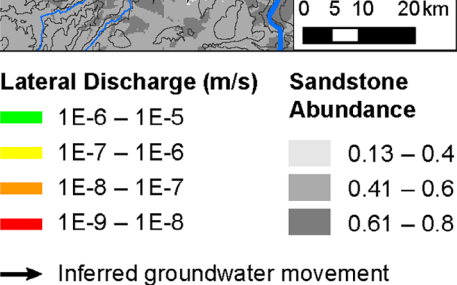
and in-turn the mean age of groundwater discharge. Haitjema and Mitchell-Bruker (2005) introduced a simple decision criteria to estimate if the water table in the region is topography- or recharge-controlled (Equation 6).

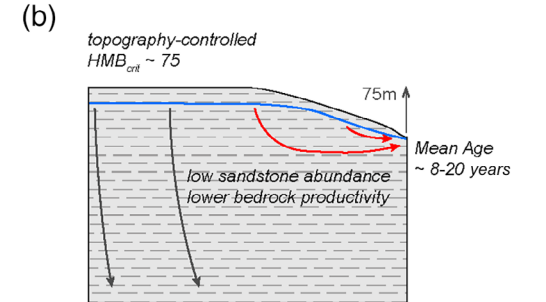
$$HMB_{crit} = \frac{RL^2}{mKHd},$$
 (6)

where R is the average groundwater recharge rate, L is the average distance between surface waters, m is a shape factor (assumed to be 16), K is the average hydraulic conductivity, H is the aquifer thickness and d is the maximum distance between the surface water level and ground elevation. Where $HMB_{crit} > 1$, the water table is likely to be topography-controlled, and where $HMB_{crit} < 1$, the water table is likely to be recharge-controlled.

For the study area, we used first-order estimates of groundwater recharge from provincial mapping (Klassen & Liggett, 2019) and a summary of hydraulic properties for the Paskapoo formation (Hughes et al., 2017). The aquifer geometry terms (H and d in Equation 6) were approximated from ground surface topography. Where the landscape has lower relief and less sandstone abundance (Figure 5b), the water table is topographically controlled







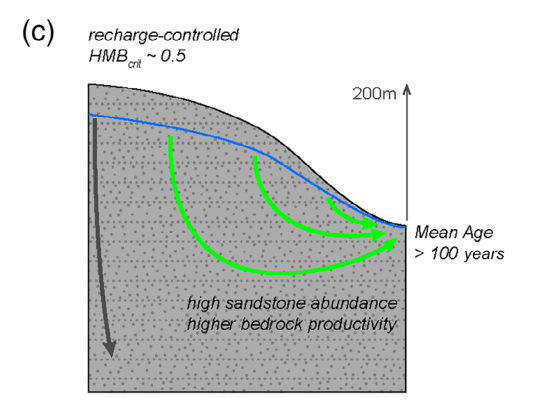


FIGURE 5 (a) Modelled groundwater discharge to each river compared to the abundance of sandstone (Babakhani et al., 2019) of the uppermost bedrock. Arrows depict the inferred groundwater flow that would support river segments with a higher amount of groundwater discharge, colour-coded to the lateral discharge flux. Conceptualizations of groundwater circulation near rivers are shown in (b) and (c) for low relief and higher relief landscapes, respectively. The water table elevation criteria (HMB_{crit}) of Haitjema and Mitchell-Bruker (2005) is shown for topographic form that has been generalized from locations shown in (a)

WILEY 11 of 15 well with our deterministic fit of 100.3 years and suggests that modelled mean age is resistive to a 50% change in ²²²Rn concentration. While the Monte Carlo analysis does not directly evaluate groundwater discharge estimates, we found a wider range of modelled groundwater discharge does not alter the interpretation of groundwater circulation for this region, and yields modelled mean age of groundwater discharge that agrees with the limited isotopic tracer data for ³H concentrations (low and groundwater verv concentrations). Groundwater discharge estimates are sensitive to the gas exchange velocity (k in Equation (2), the assumed groundwater concentration of ²²²Rn (Atkinson et al., 2015), and possibly the hyporheic and broader parafluvial zones (Cartwright et al., 2014). For the gas exchange velocity, parameter uncertainty has been shown to lead to relatively minor variation in modelled groundwater discharge using a

(HMB $_{crit} \sim 75$) and baseflow source aguifer units are a combination of river valley sediments and lower productivity bedrock. In these areas, more localized ground circulation appears to occur with a younger modelled mean age for groundwater discharge. However, where relief and sandstone abundance are greater (Figure 5c), the water table is more recharge-controlled (HMB_{crit} \sim 0.5) and the mean groundwater age discharging to rivers is greater. Again, landscape relief is indicative of aguifer thickness, river incision and bedrock productivity. The combination of simple landscape attributes (Carlier et al., 2019) and a relatively low-cost sampling program helped efficiently develop a conceptual model of groundwater circulation that can be further investigated and refined.

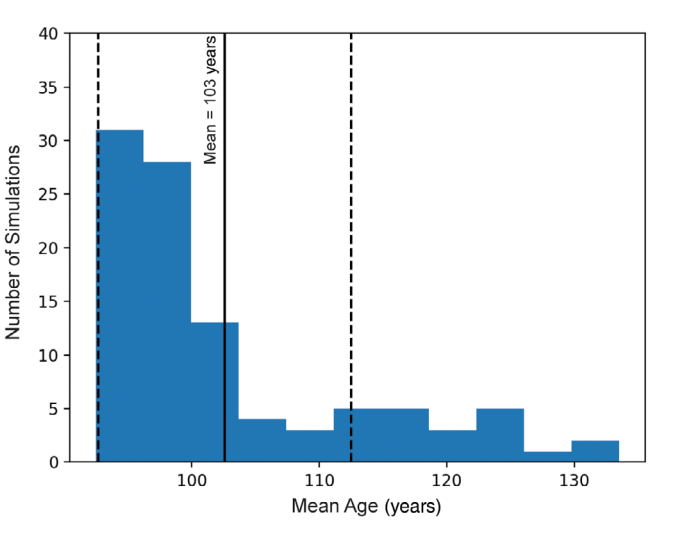
4.3 Limitations of the approach

Modelling groundwater discharge and mean age have significant uncertainty due to the unknown parameters, and in this study, the sparse isotopic tracer data for groundwater. To explore the effect of uncertainty in the estimated groundwater discharge on the estimate of groundwater mean age, we perform a Monte Carlo analysis for the Little Smoky River. Random error is added to the ²²²Rn concentrations and the full groundwater discharge and groundwater age estimation routine is carried out (Equation (7)).

$$\hat{d} = d_o + \epsilon, \tag{7}$$

where \hat{d} is the noisy data realization, ϵ random error with a mean of zero and a standard deviation of 50% of the analysed value d_0 . We performed the full inversion on 100 random realizations of ²²²Rn concentration. A histogram of the resulting modelled mean age distribution is given in Figure 6, which has a mean age of 103 years and standard deviation of 10 years. These Monte Carlo results compare

full Bayesian analysis (Beisner et al., 2018). Our gas exchange velocity is calculated using the relationships developed by Raymond et al. (2012), which account for the specific gas of interest and water temperature. For hyporheic exchange, we acknowledge that not including the term in Equation (2) could cause groundwater discharge to be overestimated when fitting with ²²²Rn (Cartwright et al., 2014; Cook et al., 2006). Although the relatively low modelled groundwater discharge values rates are driven by low ²²²Rn concentrations, we are confident that the rivers are predominately gaining groundwater based on the Q_{min}/Q_{50} values (approx. BFI). The subtle variation in modelled downstream groundwater discharge is intended to develop a conceptualization of the groundwater system, and the model adequately captures both the total river discharge and ²²²Rn concentrations. Realizing that the modelled groundwater discharge does not differentiate between local (including the hyporheic and parafluvial zones) and regional groundwater sources, we in-turn consider the modelled mean age and other isotopic tracer data. Together, the measured data and modelled results indicate two of the three rivers have baseflow sources with a mean age greater than 100 years (i.e. likely not the hyporheic zone).



The modelled mean age of groundwater discharge determined from these river surveys is not intended to be an absolute determination of mean age, but rather to provide a useful metric to assess the relative age in each river and an indication of the groundwatershed age (Haitjema, 1995). Relying on the historic input of SF₆ and ³H concentrations (Figure 2a) neglects any variability of SF₆ and ³H in precipitation that would create more unique input functions for the region. However, the modelled mean age in this study provides a general indication of the circulation time (likely better than order of magnitude) that is useful for first-order knowledge of groundwater conditions. With knowledge of the baseflow sources, and the relative depth and length scale of active groundwater circulation, conceptual models can be built. The true mean age of the groundwater discharge would be expected to change along each reach, in response to spatial variation in the hydrogeological system. It is also important to note that we are comparing the groundwater systems at a single snapshot in time. The mean age of groundwater discharge in rivers should change seasonally as different hydrology processes are active. Here, we sampled during

FIGURE 6 Histogram of estimated mean age for random realizations of ²²²Rn data. The Monte Carlo analysis was completed for the Little Smoky River



baseflow conditions, when deep groundwater discharge should be the dominant source of water. There is limited groundwater data, and we assume that groundwater chemistry of these deeper flowpaths would be relatively stable. Thus, our comparison is suitable for understanding the long-term differences in deep groundwater discharge to the streams.

The modelled mean age would also be expected to change based upon the assumed age distribution (Abrams & Haitjema, 2018) as shown in Table 2. However, the similarity of the ages using the exponential and dispersion age distributions is consistent with previous work showing the mean age is relatively robust to differences in assumed age distribution (Gardner et al., 2016; Solomon et al., 2015). In Figure 7, an indication of the model sensitivity to changes in mean age of groundwater assuming an exponential mixing model in the Little Smoky River is shown. It is apparent that SF₆ (Figure 7a) is far less sensitive to groundwater age than ³H (Figure 7b) at the modelled discharge rates (Figure 7c), likely due to re-equilibration to the atmosphere. In addition, it is clear that the ³H in particular allows us to clearly distinguish water with age differences of 50-100 years, which appears to be important for the region of study. Two of the river systems had modelled mean age around 100 years and one was closer to 10 years.

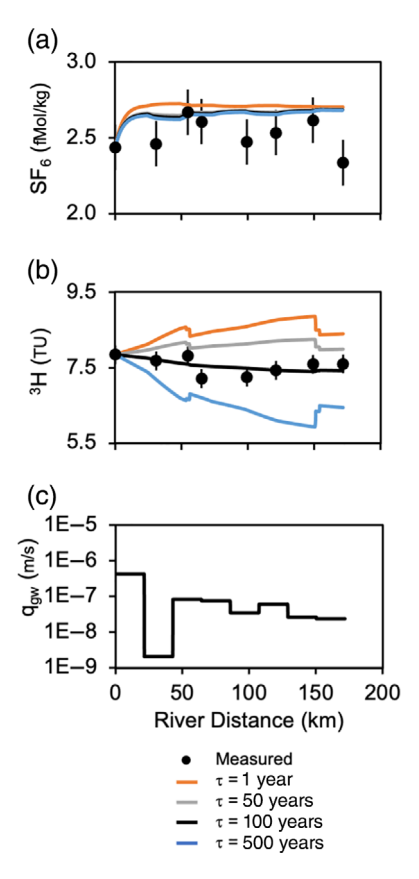


FIGURE 7 Sensitivity of modelled SF₆ and 3 H concentrations in (a) and (b) to the residence time (τ) for modelled groundwater discharge rates (c). The sensitivity analysis was completed for the Little Smoky River

5 | CONCLUSIONS

We used a suite of environmental tracers sampled from three rivers to gain an understanding of the groundwater conditions for a large area. With only knowledge of the physiography, formation-scale bedrock geology and the hydrometric record of the river, synoptic sampling of the rivers led to a plausible conceptual model based on observations. We found that benchland areas with higher topographic relief and increased sandstone abundance had hydrogeological conditions that favoured deeper groundwater circulation with a modelled mean age greater than 100 years from recharge to discharge. Lower relief areas, which coincide with transition in bedrock formations, appeared to have much shorter (and shallower) groundwater circulation. Concurrent lithologic modelling of the sandstone abundance of the bedrock supports the groundwater conditions inferred from the results of river sampling. This study demonstrates that under certain conditions rivers can be used as an easily accessible location to sample a distribution of groundwater flow paths, resulting in an efficient approach to generate first-order knowledge of groundwater conditions for a large area. Field work and the financial requirement to support this approach would be approximately equivalent to drilling a single borehole and installing a monitoring well. Thus, where few classical observation points exist and knowledge is limited, synoptic sampling of rivers can be used to develop scientifically defensible conceptual models at a comparable scale to regional planning and resource management.

ACKNOWLEDGEMENTS

The authors thank the Alberta Geological Survey for supporting the field work and laboratory analyses, and Alberta Environment and Parks for sampling the publicly available groundwater monitoring well in the study area. We thank the three reviewers comments and suggestions that helped better articulate the applicability of this research.

DATA AVAILABILITY STATEMENT

The complete laboratory analyses results can be found in Alberta Geological Survey Report 98, available at https://ags.aer.ca/publications/REP 98.html (Smerdon et al., 2019).

ORCID

Brian D. Smerdon https://orcid.org/0000-0003-2923-1980
W. Payton Gardner https://orcid.org/0000-0003-0664-001X

REFERENCES

Abrams, D., & Haitjema, H. (2018). How aquifer characteristics of a watershed affect transit time distributions of groundwater. *Groundwater*, 56(4), 517–520. https://doi.org/10.1111/gwat.12788

Alberta Environment and Parks (2019). Groundwater Observation Well Network. Retrieved from https://www.alberta.ca/groundwater-observation-well-network.aspx

Alessi, D. S., Zolfaghari, A., Kletke, S., Gehman, J., Allen, D. M., & Goss, G. G. (2017). Comparative analysis of hydraulic fracturing wastewater practices in unconventional shale development: Water sourcing, treatment, and disposal practices. *Canadian Water Resources Journal*, 42(2), 105–121. https://doi.org/10.1080/07011784.2016.1238782

SMERDON AND GARDNER WILEY 13 of 15

- Allen, D. M., Schuurman, N., Deshpande, A., & Scibek, J. (2008). Data integration and standardization in cross-border hydrogeological studies: A novel approach to hydrostratigraphic model development. *Environmental Geology*, 53, 1441–1453. https://doi.org/10.1007/s00254-007-0753-3
- Atkinson, A. P., Cartwright, I., Gilfedder, B. S., Hoffmann, H., Unland, N. P., Cendón, D. I., & Chisari, R. (2015). A multi-tracer approach to quantifying groundwater inflows to an upland river; assessing the influence of variable groundwater chemistry. *Hydrological Processes*, 29, 1–12. https://doi.org/10.1002/hyp.10122
- Atkinson, L. A., & Hartman, G. M. D. (2017). 3D rendering of the regional stratigraphy of Paleogene-Quaternary sediments in west-central Alberta; Alberta Energy Regulator/Alberta Geological Survey Report 93. Retrieved from http://ags.aer.ca/document/REP/REP 93.pdf.
- Babakhani, M., Mei, S., Atkinson, L. A., & Smerdon, B. D. (2019). 3D property modelling of the bedrock hydrostratigraphy in the Fox Creek area, west-central Alberta; Alberta Energy Regulator/Alberta Geological Survey Open File Report 2019-03. Retrieved from https://ags.aer.ca/publications/OFR_2019_03.html
- Ballentine, C. J., Burgess, R., & Marty, B. (2002). Tracing fluid origin and interaction in the crust. In D. Porcelli, C. J. Ballentine, & R. Wieler (Eds.), Noble gases in geochemistry and cosmochemistry 47 (pp. 539– 614). Mineralogical Society of America.
- Barthel, R. (2014). HESS opinions: Integration of groundwater and surface water research: An interdisciplinary problem? Hydrology and Earth System Sciences, 18, 2615–2628. https://doi.org/10.5194/hess-18-2615-2014
- Batlle-Aguilar, J., Harrington, G. A., Leblanc, M., Welch, C., & Cook, P. G. (2014). Chemistry of groundwater discharge inferred from longitudinal river sampling. Water Resources Research, 50(2), 1550–1568. https:// doi.org/10.1002/2013WR013591
- Beisner, K. R., Gardner, W. P., & Hunt, A. G. (2018). Geochemical characterization and modeling of regional groundwater contributing to the Verde River, Arizona between Mormon Pocket and the USGS Clarkdale gage. *Journal of Hydrology*, 564, 99–114. https://doi.org/10.1016/j.jhydrol.2018.06.078
- Bloomfield, J. P., Allen, D. J., & Griffiths, K. J. (2009). Examining geological controls on baseflow index (BFI) using regression analysis: An illustration from the Thames Basin, UK. *Journal of Hydrology*, 373, 164–176. https://doi.org/10.1016/j.jhydrol.2009.04.025
- Bredehoeft, J. (2005). The conceptualization model problem surprise. *Hydrogeology Journal*, 13, 37–36. https://doi.org/10.1007/s10040-004-0430-5
- Burns, E. R., Bentley, L. R., Hayashi, M., Grasby, S. E., Hamblin, A. P., Smith, D. G., & Wozniak, P. R. J. (2010). Hydrogeological implications of paleo-fluvial architecture for the Paskapoo formation, SW Alberta, Canada: A stochastic analysis. *Hydrogeology Journal*, 18(6), 1375–1390. https://doi.org/10.1007/s10040-010-0608-y
- Carlier, C., Wirth, S. B., Cochand, F., Hunkeler, D., & Brunner, P. (2019). Exploring geological and topographical controls on low flows with hydrogeological models. *Groundwater*, 57(1), 48–62. https://doi.org/ 10.1111/gwat.12845
- Cartwright, I., Hofmann, H., Gilfedder, B., & Smyth, B. (2014). Understanding parafluvial exchange and degassing to better quantify groundwater inflows using 222Rn: The King River, southeast Australia. Chemical Geology, 380, 48-60. https://doi.org/10.1016/j.chemgeo.2014.04.009
- Cook, P. G. (2015). Quantifying river gain and loss at regional scales. *Journal of Hydrology*, 531(Part 3), 749–758. https://doi.org/10.1016/j. jhydrol.2015.10.052
- Cook, P. G., & Herczeg, A. L. (2000). Environmental tracers in subsurface hydrology (p. 529). Springer. https://doi.org/10.1007/978-1-4615-4557-6
- Cook, P. G., Lamontagne, S., Berhane, D., & Clark, J. F. (2006). Quantifying groundwater discharge to Cockburn River, southeastern Australia,

- using dissolved gas tracers 222Rn and SF6. Water Resources Research, 42, W10411. https://doi.org/10.1029/2006WR004921
- Cools, J., Meyus, Y., Woldeamlak, S. T., Batelaan, O., & de Smedt, F. (2006). Large-scale GIS-based hydrogeological modeling of Flanders: A tool for groundwater management. *Environmental Geology*, 50, 1201–1209. https://doi.org/10.1007/s00254-006-0292-3
- Dawson, F. M., Kalkreuth, W. D., & Sweet, A. R. (1994). Stratigraphic and coal resource potential of the Upper Cretaceous to Tertiary strata of northwestern Alberta. Geological Survey of Canada Bulletin, 466, 67.
- Dunkle, K. M., Anderson, M. P., & Hart, D. (2015). New ways of using well construction reports for hydrostratigraphic analyses. *Groundwater*, 54(1), 126–130. https://doi.org/10.1111/gwat.12326
- Enemark, T., Peeters, L. J. M., Mallants, D., & Batelaan, O. (2019). Hydrogeological conceptual model building and testing: A review. *Journal of Hydrology*, 569, 310–329. https://doi.org/10.1016/j.jhydrol. 2018.12.007
- Environment and Climate Change Canada. (2018). HYDAT database; Environment and Climate Change Canada. Retrieved from https://collaboration.cmc.ec.gc.ca/cmc/hydrometrics/www/.
- Fanti, F., & Catuneanu, O. (2009). Stratigraphy of the Upper Cretaceous Wapiti formation, west-central Alberta, Canada. *Canadian Journal of Earth Sciences*, 46(4), 263–286. https://doi.org/10.1139/E09-020
- Frappart, F., & Ramillien, G. (2018). Monitoring groundwater storage changes using the Gravity Recovery and Climate Experiment (GRACE) satellite mission: A review. *Remote Sensing*, 10(6), 829. https://doi.org/ 10.3390/rs10060829
- Gardner, W. P., Harrington, G. A., Solomon, D. K., & Cook, P. G. (2011).
 Using terrigenic ⁴He to identify and quantify regional groundwater discharge to streams. Water Resources Research, 47(6), W06523. https://doi.org/10.1029/2010WR010276
- Gardner, W. P., Hokr, M., Shao, H., Balvin, A., Kunz, H., & Wang, Y. (2016). Investigating the age distribution of fracture discharge using multiple environmental tracers, Bedrichov Tunnel, Czech Republic. *Environmental Earth Sciences*, 75, 1374. https://doi.org/10.1007/s12665-016-6160-x
- Grasby, S. E., Betcher, R. N., Maathuis, H., & Wozniak, P. R. J. (2014). Chapter 10: Plains region. In A. Rivera (Ed.), Canada's groundwater resources (pp. 360–413). Fitzhenryand Whiteside.
- Grasby, S. E., Chen, Z., Hamblin, A. P., Wozniak, P. R. J., & Sweet, A. R. (2008). Regional characterization of the Paskapoo bedrock aquifer system, southern Alberta. *Canadian Journal of Earth Sciences*, 45(12), 1501–1516. https://doi.org/10.1139/E08-069
- Gustard, A., Bullock, A., & Dixon, J. M. (1992). Low flow estimation in the United Kingdom (Institute of Hydrology Report No. 108) (p. 88. Retrieved from). Institute of Hydrology. http://nora.nerc.ac.uk/id/eprint/6050/ 1/IH_108.pdf
- Haitjema, H. M. (1995). On the residence time distribution in idealized groundwatersheds. *Journal of Hydrology*, 172, 127–146. https://doi. org/10.1016/0022-1694(95)02732-5
- Haitjema, H. M., & Mitchell-Bruker, S. (2005). Are water tables a subdued replica of the topography? *Groundwater*, 43(6), 781–786. https://doi.org/10.1111/j.1745-6584.2005.00090.x
- Hamblin, A. P. (2004). Paskapoo-Porcupine Hills formations in western Alberta: Synthesis of regional geology and resource potential. *Geological Survey of Canada, Open File*, 4679, 30.
- Harrington, G. A., Payton, G. W., & Munday, T. J. (2014). Tracking ground-water discharge to a large river using tracers and geophysics. *Groundwater*, 52(6), 837–852. https://doi.org/10.1111/gwat.12124
- Hathway, B. (2011). Late Maastrichtian paleovalley systems in west-central Alberta: Mapping the Battle formation in the subsurface. Bulletin of Canadian Petroleum Geology, 59(3), 195–206. https://doi.org/10.2113/gscpgbull.59.3.195
- Hokanson, K. J., Mendoza, C. A., & Devito, K. J. (2019). Interactions between regional climate, surficial geology, and topography: Characterizing shallow groundwater systems in subhumid, low-relief



- landscapes. Water Resources Research, 55(1), 284-297. https://doi.org/10.1029/2018WR023934
- Huang, J., Pavlic, G., Rivera, A., Palombi, D., & Smerdon, B. (2016). Mapping groundwater storage variations with GRACE: A case study in Alberta, Canada. *Hydrogeology Journal*, 24, 1663–1680. https://doi.org/10.1007/s10040-016-1412-0
- Hughes, A. T., Smerdon, B. D., & Alessi, D. S. (2017). Hydraulic properties of the Paskapoo formation in west-central Alberta. *Canadian Journal of Earth Sciences*, 54(8), 883–892. https://doi.org/10.1139/cjes-2016-0164
- IAEA/WMO. (2016). Global network of isotopes in precipitation. The GNIP Database. Retrieved from http://www.iaea.org/water
- Irish, E. J. W. (1970). The Edmonton group of south-Central Alberta. *Bulletin of Canadian Petroleum Geology*, 18(2), 125–155.
- Jasechko, S. (2016). Partitioning young and old groundwater with geochemical tracers. Chemical Geology, 427, 35–42. https://doi.org/10.1016/j.chemgeo.2016.02.012
- Jørgensen, F., Møller, R. R., Nebel, L., Jensen, N.-P., Christiansen, A. V., & Sanderson, P. B. E. (2013). A method for cognitive 3D geological voxel modelling of AEM data. Bulletin of Engineering Geology and the Environment, 72, 421–432. https://doi.org/10.1007/s10064-013-0487-2
- Klassen, J., & Liggett, J.E. (2019). First-order groundwater availability assessment for the upper Peace region; Alberta Energy Regulator/Alberta Geological Survey Open File Report 2019-10. Retrieved from https://ags.aer.ca/publications/OFR 2019 10.html.
- Knappe, E., Bendick, R., Martens, H. R., Argus, D. F., & Gardner, W. P. (2019). Downscaling vertical GPS observations to derive watershedscale hydrologic loading in the northern Rockies. Water Resources Research, 55(1), 391–401. https://doi.org/10.1029/2018WR023289
- Knight, R., Smith, R., Asch, T., Abraham, J., Cannia, J., Viezzoli, A., & Fogg, G. (2018). Mapping aquifer systems with airborne electromagnetics in the Central Valley of California. *Groundwater*, 56(6), 893–908. https://doi.org/10.1111/gwat.12656
- Lee, R. W., & Hollyday, E. F. (1991). Use of radon measurements in Carters Creek, Maury County, Tennessee to determine location and magnitude of groundwater seepage. In L. C. S. Gundersen & R. B. Wanty (Eds.), Field studies of radon in rocks, soils, and water (pp. 237–242). C.K. Smolev.
- Lekula, M., Lubczynski, M. W., & Shemang, E. M. (2018). Hydrogeological conceptual model of large and complex sedimentary aquifer systems— Central Kalahari Basin. *Physics and Chemistry of the Earth, Parts A/B/C*, 106, 47–62. https://doi.org/10.1016/j.pce.2018.05.006
- Leray, S., Engdahl, N. B., Massoudieh, A., Bresciani, E., & McCallum, J. (2016). Residence time distributions for hydrologic systems: Mechanistic foundations and steady-state analytical solutions. *Journal of Hydrology*, 543, 67–87. https://doi.org/10.1016/j.jhydrol.2016.01.068
- Lyster, S., & Andriashek, L. D. (2012). Geostatistical rendering of the architecture of hydrostratigraphic units within the Paskapoo formation, central Alberta. Energy Resources Conservation Board Bulletin, 66, 115.
- MacCormack, K. E., Berg, R. C., Kessler, H., Russell, H. A. J., & Thorleifson, L. H. (2019). 2019 synopsis of current three-dimensional geological mapping and modelling in geological survey organizations. Alberta Energy Regulator/Alberta Geological Survey Special Report 112. Retrieved from https://ags.aer.ca/publications/SPE_112.html.
- Maloszewski, P., & Zuber, A. (1982). Determining the turnover time of groundwater systems with the aid of environmental tracers. *Journal of Hydrology*, 57(3), 207–231. https://doi.org/10.1016/0022-1694(82) 90147-0
- McCallum, J. L., Cook, P. G., Berhane, D., Rumpf, C., & McMahon, G. A. (2012). Quantifying groundwater flows to streams using differential flow gaugings and water chemistry. *Journal of Hydrology*, 416–417, 118–132. https://doi.org/10.1016/j.jhydrol.2011.11.040
- Mei, S. (2019). Three-dimensional property modelling of the Scollard, Paskapoo and Porcupine Hills formations in southwest Alberta. Alberta Energy Regulator/Alberta Geological Survey Open File Report

- 2019-05. Retrieved from https://ags.aer.ca/publications/OFR_2019_ 05.html
- Moya, C. E., Raiber, M., & Cox, M. E. (2014). Three-dimensional geological modelling of the Galilee and central Eromanga basins, Australia: New insights into aquifer/aquitard geometry and potential influence of faults on inter-connectivity. *Journal of Hydrology: Regional Studies*, 2, 119–139. https://doi.org/10.1016/j.ejrh.2014.08.007
- NOAA. (2018). Combined sulfur hexaflouride data from the NOAA/ESRL global monitoring division. Retrieved from https://gml.noaa.gov/hats/combined/SF6.html.
- Quartero, E. M., Leier, A. L., Bentley, L. R., & Glombick, P. (2015). Basin-scale stratigraphic architecture and potential Paleocene distributive fluvial systems of the Cordilleran Foreland Basin, Alberta, Canada. Sedimentary Geology, 316, 26–38. https://doi.org/10.1016/j.sedgeo.2014. 11.005
- Raymond, P. A., Zappa, C. J., Butman, D., Bott, T. L., Potter, J., Mulholland, P., Laursen, A. E., McDowell, W. H., & Newbold, D. (2012). Scaling the gas transfer velocity and hydraulic geometry in streams and small rivers. *Limnology and Oceanography: Fluids and Environments*, 2(1), 41–53. https://doi.org/10.1215/21573689-1597669
- Schilling, O. S., Cook, P. G., & Brunner, P. (2019). Beyond classical observations in hydrogeology: The advantages of including exchange flux, temperature, tracer concentration, residence time, and soil moisture observations in groundwater model calibration. *Reviews of Geophysics*, 57, 146–182. https://doi.org/10.1029/2018RG000619
- Smerdon, B. D., Gardner, W. P., Harrington, G. A., & Tickell, S. J. (2012). Identifying the contribution of regional groundwater to the base-flow of a tropical river (Daly River, Australia). *Journal of Hydrology*, 464–465, 107–115. https://doi.org/10.1016/j.jhydrol.2012. 06.058
- Smerdon, B. D., Klassen, J., & Gardner, W. P. (2019). Hydrogeological characterization of the upper Cretaceous–Quaternary units in the Fox Creek area, west-central Alberta; Alberta Energy Regulator/Alberta Geological Survey, Report 98. Retrieved from https://ags.aer.ca/publications/REP_98.html
- Solomon, D. K., Genereux, D. P., Plummer, L. N., & Busenberg, E. (2010). Testing mixing models of old and young groundwater in a tropical low-land rain forest with environmental tracers. Water Resources Research, 46, W04518. https://doi.org/10.1029/2009wr008341
- Solomon, D. K., Gilmore, T. E., Solder, J. E., Kimball, B., & Genereux, D. P. (2015). Evaluating an unconfined aquifer by analysis of age-dating tracers in stream water. Water Resources Research, 51 (110, 8883–8899. https://doi.org/10.1002/2015WR017602
- Stampoulis, D., Reager, J. T., David, C. H., Andreadis, K. M., Famiglietti, J. S., Farr, T. G., Trangsrud, A. R., Basilio, R. R., Sabo, J. L., Osterman, G. B., Lundgren, P. R., & Liu, Z. (2019). Model-data fusion of hydrologic simulations and GRACE terrestrial water storage observations to estimate changes in water table depth. Advances in Water Resources, 128, 13–27. https://doi.org/10.1016/j.advwatres.2019. 04.004
- Stolp, B. J., Solomon, D. K., Suckow, A., Vitvar, T., Rank, D., Aggarwal, P. K., & Han, L. F. (2010). Age dating base flow at springs and gaining streams using helium-3 and tritium: Fischa-Dagnitz system, southern Vienna Basin, Austria. Water Resources Research, 46, W07503. https://doi.org/10.1029/2009WR008006
- Tóth, J. (1970). A conceptual model of the groundwater regime and the hydrogeologic environment. *Journal of Hydrology*, 10(2), 164–176. https://doi.org/10.1016/0022-1694(70)90186-1
- Wang, T., Hamann, A., Spittlehouse, D., & Carroll, C. (2016). Locally down-scaled and spatially customizable climate data for historical and future periods for North America. PLoS One, 11(6), e0156720. https://doi.org/10.1371/journal.pone.0156720
- Welch, L. A., & Allen, D. M. (2012). Consistency of groundwater flow patterns in mountainous topography: Implications for valley bottom water

replenishment and for defining groundwater flow boundaries. *Water Resources Research*, 48, W05526. https://doi.org/10.1029/2011WR010901

SUPPORTING INFORMATION

Additional supporting information may be found in the online version of the article at the publisher's website.

How to cite this article: Smerdon, B. D., & Gardner, W. P. (2022). Characterizing groundwater flow paths in an undeveloped region through synoptic river sampling for environmental tracers. *Hydrological Processes*, *36*(1), e14464. https://doi.org/10.1002/hyp.14464